POLARIZATION OBSERVABLES IN DALITZ DECAYS $\chi_{cJ} \to J/\psi + \mu^+\mu^-$ AT THE LHC*

S.P. Baranov

P.N. Lebedev Institute of Physics, Lenin Avenue 53, Moscow 119991, Russia

(Received March 5, 2019)

We consider the production of χ_{cJ} mesons at the LHC conditions and show predictions for polarization observables for the original χ_{cJ} mesons and their decay products. We find that the polarization of χ_{cJ} and J/ψ mesons is large and shows nontrivial behavior as a function of χ_{cJ} transverse momentum. A comparison between collinear and $k_{\rm T}$-factorization predictions is presented.

DOI:10.5506/APhysPolBSupp.12.843

1. Motivation

Polarization observables play the prominent role in modern physics and can, in many cases, provide unique and crucial information on the interaction dynamics. While the predictions on the absolute production cross sections may vary significantly with the input parton densities, the renormalization and factorization scales, the quark mass values, *etc.*, the polarization is mainly sensitive to the production mechanism on its own, and so, may serve as a much better indicator of the latter.

Our present note is devoted to a theoretical analysis of the decays of χ_{c1} and χ_{c2} mesons produced in high-energy hadronic collisions

$$pp \to \chi_{cJ} + X\,; \qquad \chi_{cJ} \to J/\psi + l^+l^-\,; \qquad J/\psi \to l^+l^-\,. \tag{1}$$

This study was inspired by a distinctive identification [1] of χ_{c1} and χ_{c1} Dalitz decays by the LHCb Collaboration at CERN. Therefore, we will be basically addressing to the LHCb conditions. LHCb imposes no restrictions on the transverse momenta, and this is really a big advantage in comparison with ATLAS or the CMS, where the $p_{\rm T}$ cuts translate into blind areas in the angular distributions and make the polarization analysis rather uncomfortable.

* Presented at the Diffraction and Low-x 2018 Workshop, August 26–September 1, 2018, Reggio Calabria, Italy.

In the context of χ_{cJ} Dalitz decays, one can consider three sets of polarization observables. First is the polarization of the original χ_{cJ} mesons that can be seen in the angular distributions of the resulting J/ψmesons and virtual photons. Second is the polarization of the daughter J/ψs that manifests in the angular distributions of the decay leptons. Third is the polarization of the virtual photon that can be seen in the angular distributions of the other lepton pair. We will derive theoretical predictions for these three sets of observables in the helicity and the Collins–Soper frames.

2. Theoretical framework

The theoretical analysis is greatly simplified by the fact that the production of χ_{cJ} mesons is dominated by a single channel known as the color singlet mechanism. This has been found true for both collinear [2] and k_{T}-factorization [3] approaches. Thanks to that, the theory has no free parameters and the predictions are certain. Our present calculations are based on the standard QCD perturbation theory and nonrelativistic bound state formalism of Refs. [4, 5].

In the k_{T}-factorization approach [6], we consider the partonic subprocess

$$g^* + g^* \to \chi_{cJ}\,, \qquad J = 0, 1, 2 \tag{2}$$

that represents the leading-order (LO) QCD contribution. In the case of collinear factorization, the leading order is represented by a $2 \to 2$ subprocess

$$g + g \to \chi_{cJ} + g, q\,, \qquad J = 0, 1, 2 \tag{3}$$

as the $2 \to 1$ subprocess (2) would lead to unacceptable unphysical δ-like p_{T} distributions. The corresponding Feynman diagrams are shown in Fig. 1.

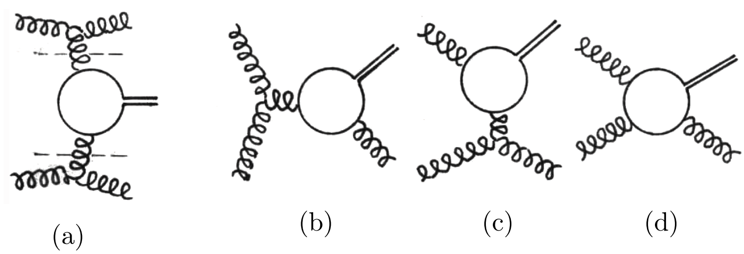

Fig. 1. Feynman diagrams representing the hadronic production of χ_{cJ} mesons in the k_{T}-factorization (a) and leading order collinear (b)–(d) approaches. The central part of (a) represents the hard partonic subprocess (2); the upper and the lower parts of the diagram represent the evolution of gluon densities.

The amplitudes of the partonic subprocesses (2) and (3) contain spin projection operators that guarantee the proper quantum numbers of the $c\bar{c}$-bound states. The details of calculations are explained in Refs. [7, 8]. For the sake of definiteness, we only present here our parameter setting. Throughout this note, we use the leading-order MSTW parametrization [9] for collinear gluon density. For the unintegrated density, we use the parametrization A0 from Ref. [10]. The latter is derived as a numerical fit to the available F_2 data and is based on the CCFM equation [11].

The renormalization and factorization scales are set to $\mu_{\rm R}^2 = \mu_{\rm F}^2 = m_\chi^2 + p_{\rm T}^2$, the charmed quark mass $m_c = m_\chi/2 = 1.77$ GeV, and the value of the χ_{cJ} wave function $|\mathcal{R}'_\chi(0)|^2 = 0.075$ GeV^3 is taken from the potential model of Ref. [12]. (The χ_{c1} and χ_{c2} wave functions are taken equal; their numerical values have, however, no effect on the polarization observables). The integration over the final-state phase space is restricted to the rapidity interval specified by the LHCb Collaboration [1]: $2.0 < y_\chi < 4.9$.

The decays $\chi_{cJ} \to J/\psi + \gamma^*$ are assumed to be dominated by electric dipole E1 transitions. The corresponding amplitudes read [13, 14]

$$\mathcal{A}(\chi_{c1}(p) \to J/\psi(p-k) + \gamma(k)) \;\propto\; \epsilon^{\mu\nu\alpha\beta}\, k_\mu\, \varepsilon_\nu^{(\chi_{c1})}\, \varepsilon_\alpha^{(\psi)}\, \varepsilon_\beta^{(\gamma)}\,, \tag{4}$$

$$\mathcal{A}(\chi_{c2}(p) \to J/\psi(p-k) + \gamma(k)) \;\propto\; p^\mu\, \varepsilon^{\alpha\beta}_{(\chi_{c2})}\, \varepsilon_\alpha^{(\psi)} \left[k_\mu\, \varepsilon_\beta^{(\gamma)} - k_\beta\, \varepsilon_\mu^{(\gamma)}\right], \tag{5}$$

where p, k, and $p-k$ indicate the momenta of the initial χ_{cJ} meson and its daughter particles, and $\varepsilon^{(\chi_{c2})}$, $\varepsilon^{(\chi_{c1})}$, $\varepsilon^{(\psi)}$, $\varepsilon^{(\gamma)}$ stand for the respective polarization tensor and vectors. Further on, the decays $J/\psi \to \mu^+\mu^-$ and $\gamma^* \to \mu^+\mu^-$ can be described with the spin density matrices written in terms of the outgoing lepton momenta q^+, q^-, k^+, k^-

$$\varepsilon_\alpha^{(\psi)}\varepsilon_\beta^{(\psi)*} \;=\; 3\left(\left(q_\alpha^+ q_\beta^- + q_\alpha^- q_\beta^+\right)/m_\psi + g_{\alpha\beta}/2\right), \tag{6}$$

$$\varepsilon_\alpha^{(\gamma)}\varepsilon_\beta^{(\gamma)*} \;=\; 3\left(\left(k_\alpha^+ k_\beta^- + k_\alpha^- k_\beta^+\right)/m_{\mu\mu} + g_{\alpha\beta}/2\right). \tag{7}$$

3. Numerical results

First, we show the relative fractions of the different helicity states of χ_{c1} and χ_{c2} mesons, see Fig. 2. The similarity of the collinear and $k_{\rm T}$-factorization results may look rather surprising, in view of the different diagrams employed in these two calculations. However, the difference is less important than it seems at first sight. The intermediate gluons in 'collinear' diagrams (internal lines in Fig. 1 (b)–(d)) bear strong resemblance to the initial gluons in the $k_{\rm T}$-factorization approach (Fig. 1 (a)): they are off-shell, have nonzero transverse momentum and longitudinal component in the polarization vector, *etc.* The emission of the final-state gluon in Fig. 2 (c) is included in the k_T-factorization approach as a part of the gluon density evolution. It rather looks like referring to the same physics under different names. What is taken as the initial gluon evolution in the k_T-factorization approach, constitutes part of the hard subprocess in the collinear scheme.

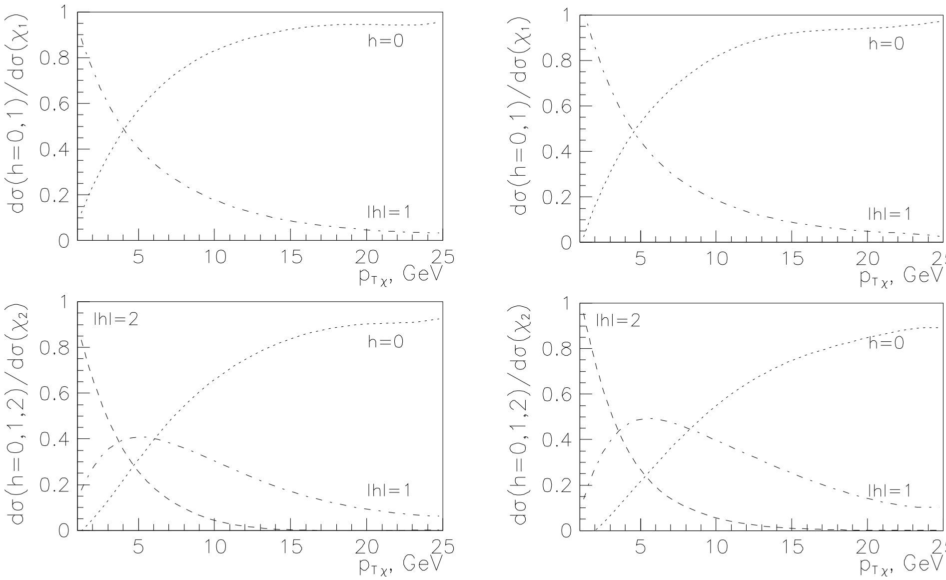

Fig. 2. Fractions of the different χ_{cJ} helicity states as seen in the helicity frame. Upper panels, χ_{c1} mesons; lower panels, χ_{c2} mesons. Dotted curves, $h = 0$; dash-dotted curves, $|h| = 1$; dashed curves, $|h| = 2$. Left panels, k_T-factorization; right panels, collinear factorization.

Regarding the results on their own, one can easily identify several intervals in p_T, each corresponding to the dominance of a particular helicity state. The high-p_T region is fully dominated by helicity zero states for both χ_{c1} and χ_{c2} mesons. A simple (but probably reasonable) explanation points to the relative sizes of the specific components of the polarization vector and tensor. Namely, they scale as $O(1) : O(E/m)$ for the $h = \pm 1$ and $h = 0$ states of a vector meson and $O(1) : O(E/m) : O(E^2/m^2)$ for the $h = \pm 2$, $h = \pm 1$, and $h = 0$ states of a tensor meson.

The polarizations of J/ψ mesons and virtual photons are fully determined by the polarization of the original χ_c mesons through the E1 decay amplitudes Eqs. (4), (5). We present these polarizations in terms of the decay parameter α that describes the distribution of the final-state leptons in a chosen reference frame: $\mathrm{d}\Gamma_{\mu\mu}/\mathrm{d}\cos\theta_\mu \propto 1 + \alpha \cos^2\theta_\mu$. This parameter relates to the fraction of longitudinally polarized vector particles via $\alpha = (1 - 3h_0)/(1 + h_0)$. Our predictions are displayed in Figs. 3–4.

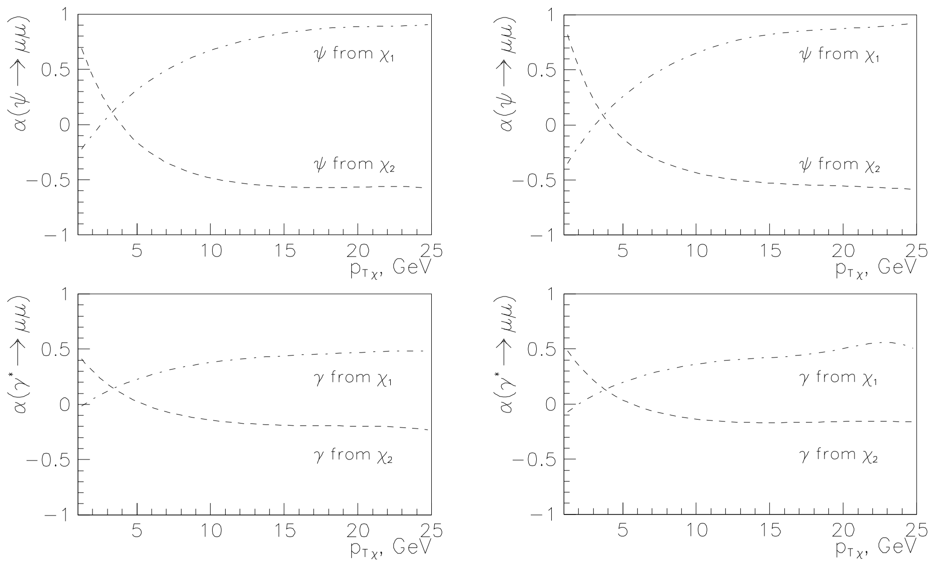

Fig. 3. J/ψ and photon polarizations in terms of the decay parameter α as seen in the helicity frame. Dash-dotted and dashed curves are for χ_{c1} and χ_{c2} decays, respectively. Left panel, k_{T}-factorization; right panel, collinear factorization.

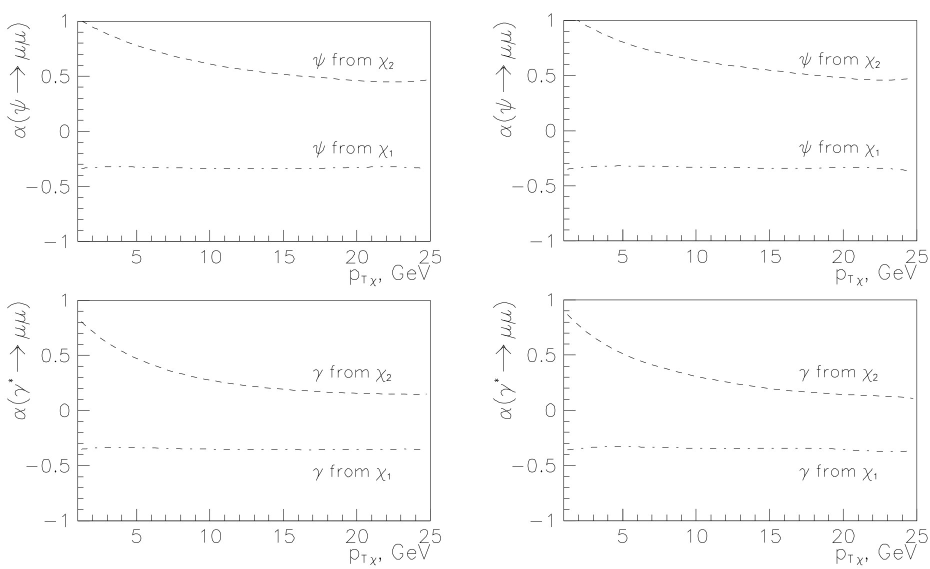

Fig. 4. J/ψ and photon polarizations in terms of the decay parameter α as seen in the Collins–Soper frame. Dash-dotted and dashed curves are for χ_{c1} and χ_{c2} decays, respectively. Left panel, k_{T}-factorization; right panel, collinear factorization.

4. Conclusions

We have considered the production of χ_{c1} and χ_{c2} mesons at the LHCb conditions and made predictions on their polarization. We notice great likeliness between the collinear and $k_{\rm T}$-factorization results, in spite of apparently different Feynman diagrams used in calculations. This fact may indicate that both approaches address the same physics under different names.

We make numerical predictions for the 'helicity' and the Collins–Soper frames. We find that the polarization of χ_{cJ} and J/ψ mesons is large and possesses nontrivial behavior as a function of χ_{cJ} transverse momentum. The high-$p_{\rm T}$ region is totally dominated by helicity zero states for both χ_{c1} and χ_{c2} mesons.

The goal of this study is to stimulate a new measurement and to provide the necessary theoretical grounds. If the statistics is not sufficient to extract the polarization parameters as smooth curves, our results may help to set an adequate binning.

This work was supported by the DESY Directorate in the framework of Moscow–DESY project on Monte Carlo implementation for HERA-LHC. Attendance to the conference was supported by the Organizing committee.

REFERENCES

[1] R. Aaij *et al.* [LHCb Collab.], *Phys. Rev. Lett.* **119**, 221801 (2017).

[2] A.K. Likhoded, A.V. Luchinsky, S.V. Poslavsky, *Phys. Rev. D* **90**, 074021 (2014).

[3] S.P. Baranov, A.V. Lipatov, N.P. Zotov, *Phys. Rev. D* **93**, 094012 (2016).

[4] G. Guberina, J. Kühn, R. Peccei, R. Rückl, *Nucl. Phys. B* **174**, 317 (1980).

[5] H. Krasemann, *Z. Phys. C* **1**, 189 (1979).

[6] L.V. Gribov, E.M. Levin, M.G. Ryskin, *Phys. Rep.* **100**, 1 (1983); E.M. Levin, M.G. Ryskin, *Phys. Rep.* **189**, 268 (1990).

[7] S.P. Baranov, *Phys. Rev. D* **66**, 114003 (2002).

[8] B. Kniehl, G. Kramer, C. Palisoc, *Phys. Rev. D* **68**, 114002 (2003).

[9] A.D. Martin, W.J. Stirling, R.S. Thorne, G. Watt, *Eur. Phys. J. C* **63**, 189 (2009).

[10] H. Jung, `http://www.desy.de/~jung/cascade/updf.html`

[11] M. Ciafaloni, *Nucl. Phys. B* **296**, 49 (1998); S. Catani, F. Fiorani, G. Marchesini, *Phys. Lett. B* **234**, 339 (1990); *Nucl. Phys. B* **336**, 18 (1990); **445**, 49 (1995).

[12] E.J. Eichten, C. Quigg, *Phys. Rev. D* **52**, 1726 (1995).

[13] A.V. Batunin, S.R. Slabospitsky, *Phys. Lett. B* **188**, 269 (1987).

[14] P. Cho, M. Wise, S. Trivedi, *Phys. Rev. D* **51**, R2039 (1995).

[15] M. Tanabashi *et al.* [Particle Data Group], *Phys. Rev. D* **98**, 030001 (2018).